Proceedings of AJTEC2011
ASME/JSME 2011 8th Thermal Engineering Joint Conference
March 14-17, 2011, Honolulu, Hawaii, USA

AJTEC2011-44218

SIMULTANEOUS HEAT TRANSFER AND PRESSURE DROP MEASUREMENTS FOR A HORIZONTAL MICRO-TUBE

Lap Mou Tam
Department of Electromechanical Engineering, Faculty of Science and Technology, University of Macau, Av. Padre Tomás Pereira, Taipa, Macau, China.
Institute for the Development and Quality, Macau.

Hou Kuan Tam
Department of Electromechanical Engineering, Faculty of Science and Technology, University of Macau, Av. Padre Tomás Pereira, Taipa, Macau, China.

Afshin J. Ghajar
School of Mechanical and Aerospace Engineering, Oklahoma State University, Stillwater, Oklahoma, USA.

ABSTRACT

Heat transfer and pressure drop measurements for horizontal macro-tubes under uniform wall heat flux boundary condition have been conducted by various researchers in recent years. From their studies, it was shown that good agreements were observed in the laminar and turbulent regions. However, for the transition region, the heat transfer and pressure drop characteristics depended on various factors, such as inlet configuration, buoyancy effect, and surface roughness. In a recent study by Tam et al. (2010), they measured the heat transfer and pressure drop simultaneously for a horizontal macro-tube with and without internally micro-fins and concluded that under the heating condition, the transition Reynolds number range for heat transfer and pressure drop were completely different. The transition Reynolds number range was documented in their research in great detail. However, for horizontal micro-tubes, there is no information in the literature on the simultaneous behavior of the heat transfer and pressure drop, especially in the transition region. In order to fill in this gap, an experimental setup was built to measure the heat transfer and pressure drop simultaneously for a horizontal micro-tube under uniform wall heat flux boundary condition. Water was used as the test fluid and the test section was a stainless steel micro-tube with 1000μm diameter. For heat transfer, the results indicated that the micro-tube had an earlier start and end of transition compared to the macro-tube and, in the turbulent region, an increase in heat transfer due to the surface roughness was observed. For friction factor under isothermal condition, the micro-tube had a narrower transition range due to the roughness compared to the macro-tube. For friction factor under heating condition, the laminar data and the start of transition were different from the isothermal case, and the effect of heating was not seen on the end of transition.

INTRODUCTION

Due to rapid advancement in fabrication techniques, the miniaturization of devices and components is ever increasing in many applications. Whether it is in the application of miniature heat exchangers, fuel cells, pumps, compressors, turbines, sensors, or artificial blood vessels, a sound understanding of fluid flow in micro-scale channels and tubes is required. Indeed, within this last decade, countless researchers have been investigating the phenomenon of fluid flow in mini-, micro-, and even nanochannels. However, previous experiments in single-phase heat transfer in micro-channels have shown a lot of disagreement with the classical behavior. No concrete conclusion regarding the adherence to macro-scale behavior has been confirmed so far. Prior reviews (Obot, 2000; Palm, 2001; Papautsky et al., 2001; Sobhan and Garimella, 2001; Rostami et al., 2002) along with recent reviews (Celata, 2004; Morini, 2004; Hestroni, 2005; Yang and Lin, 2007) have presented comprehensive information on heat transfer and fluid flow in micro-channels and micro-tubes. According to Krishnamoorthy et al. (2007), transition in micro-tubes does not compare well with any of the available macro-scale correlations. Moreover, the precise start and end of the transition region and the different factors affecting it have not been observed and discussed in the past literature.

Another major area of research in the phenomenon of fluid flow in mini- and microchannels is the friction factor. However, amidst all the investigations in mini- and microchannel flow, there seems to be a lack in the study of the flow in the transition region. One obvious question is the location of the transition region with respect to the hydraulic diameter of the channel and the roughness of the channel. To successfully understand friction factor and the location of the transition region, a systematic experimental investigation on various roughness values of micro-tubes is necessary. However, the science behind these advanced technologies seems to be controversial, especially fueled by the experimental results of the fluid flow and heat transfer at these small scales. On one hand, researchers have found that the friction factors to be below the classical laminar region theory (Choi et al., 1991; Yu et al., 1995). Meanwhile, some have reported that friction factor correlations for conventional sized tubes to be applicable for mini- and micro-tubes (Mala and Li, 1999; Kandikar et al., 2003; Li et al., 2003). However, many recent experiments on small-sized tubes and channels have observed higher friction factors than the correlations for conventional-sized tubes and channels (Zhao and Liu, 2006; Hwang and Kim, 2006; Rands et al., 2006; Celeta et al., 2006; Tang et al., 2007), and the cause of this discrepancy was attributed to surface roughness. Ghajar et al. (2010a) experimentally verified that the wrong selection of pressure sensing diaphragm lead to unrealistic results and frequently the unrealistic results were blamed to be the effect of roughness. In this study, the diaphragms selection scheme suggested by Ghajar et al. (2010a) was used.

In the literature, there is very little information on the simultaneous behavior of heat transfer and pressure drop, especially, in the transition region. Therefore, in this study, the major objectives of this research are (1) to develop an experimental setup to measure the heat transfer and pressure drop for a horizontal micro-tube under the isothermal and uniform wall heat flux boundary conditions; (2) to accurately measure the heat transfer and pressure drop in micro-tubes simultaneously and examine the effects of factors such as roughness and diameter on the overall heat transfer and pressure drop characteristics, especially, in the transition region; and (3) to examine the effect of heating on the friction factor for micro-tubes.

EXPERIMENTAL SETUP AND DATA REDUCTION

The experimentation for this study was performed using a relatively simple but highly effective apparatus. The apparatus used was designed with the intention of conducting highly accurate heat transfer and pressure drop measurements. The apparatus consists of four major components. These are the fluid delivery system, the flow meter banks, the test section assembly, and the data acquisition system. An overall schematic for the experimental test apparatus is shown in Figure 1. The fluid delivery system consists of a high pressure cylinder filled with ultra high purity nitrogen in combination with a stainless steel pressure vessel. After the working fluid passes through the apparatus, it is collected into a sealed container. The working fluid, distilled water is stored in the stainless steel pressure vessel. As the pressurized nitrogen is fed into the pressure vessel, the working fluid is forced up a stem extending to the bottom of the vessel, out of the pressure vessel, and through the flow meter array and test section.

Flow rate of the water entering the array is further regulated using a metering valve. Two Coriolis flow meters are necessary in order to accommodate different range of flow rates. Both flow meters were factory calibrated. The accuracy of the mass flow rate is within ±0.5%. After passing through the flow meter array, fluid enters the test section assembly. The test section assembly contains the test section as well as the equipment necessary for measurement of inlet and outlet fluid temperature and pressure drop. The test section is placed on a high density polyethylene (HDPE) sheet. Four adjustable bolts and a level were installed on the HDPE board to keep the test section in a horizontal position.

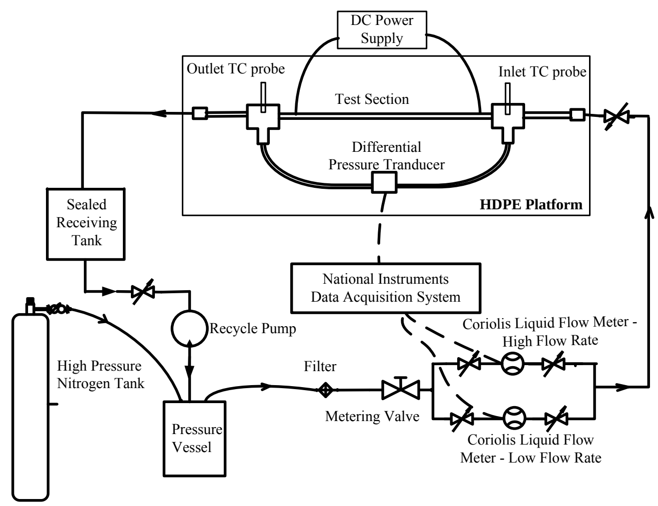

Figure 1: Schematic diagram of heat transfer and pressure drop measurement system.

In this study, the test sections included the stainless steel tubes with 1000μm and 2000μm inner diameters. The 2000μm macro-tube was used for verification of the experimental setup. The manufacturer specified an inner wall root mean square roughness of 0.41μm. Compared to the 2000μm inner diameter, the roughness was relatively small and, therefore, the effect of the roughness for the macro-tube was negligible. However, for the micro-tube, the roughness was a major factor affecting the heat transfer and pressure drop and was measured for the 1000μm micro-tube. For measuring the surface roughness, as seen in Figure 2, a Dektak 6M Stylus Surface Profilometer was used. The value of surface roughness (Ra) and the relative roughness (ε/D) was 4.3μm and 0.004308, respectively.

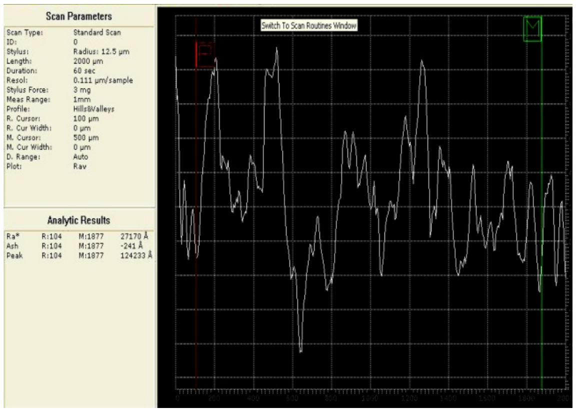

Figure 2: Roughness measured by the surface profiler.

Since the stainless steel micro-tubes in this study were purchased from an outside source, data obtained from these tubes is only as accurate as the manufacturer's specifications. In order to ensure that the data recorded was of the highest quality possible, it was deemed necessary to determine the degree of accuracy of the manufacturer's specifications. This was done by using the scanning electron microscope (SEM) for two different stainless steel tube sizes in order to check the accuracy of the manufacturer's tolerances. Figure 3 shows the SEM measurements for the two stainless tubes. The two stainless steel tubes examined had an inner diameter and tolerance of 2000±32µm and 1000±14µm, respectively. The SEM imaging of these two tubes established that the manufacturer's specifications of the tube diameters and tolerances are verifiable and dependable.

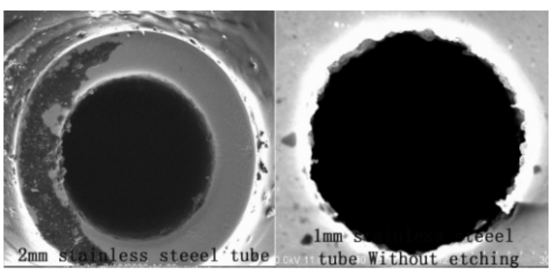

(a) (b)

Figure 3: SEM measurement of the stainless steel tubes: (a) 2000µm tube; (b) 1000µm tube.

As shown in Figure 4, electric copper wires were soldered on to the outside surface of the tubes tested. A DC power supply was used to provide the uniform wall heat flux boundary condition. For the temperature measurements, the inlet and exit bulk temperatures were measured by means of thermocouple probes (Omega TMQSS-125U-6) placed before and after the test section, respectively. Also, self-adhesive thermocouples (Omega SA1XL-T-72) were placed along the test section. All the thermocouples and thermocouple probes were calibrated by a NIST-calibrated thermocouple probe (±0.22°C) and an Omega HCTB-3030 constant temperature circulating bath. Therefore, the temperature sensors were as accurate as ±0.22°C. Figure 4 shows the arrangement of the thermocouples on the test section. The thermocouples were placed at close intervals near the entrance and at greater intervals further downstream. As the diameter of the micro-tube was small, only two surface thermocouples (TC1 and TC2) were located on the periphery of the tube at each station. After installation of the thermocouples, the micro-tube was covered by self-adhesive elastomeric insulating material. From the local peripheral wall temperature measurements at each axial location, the inside wall temperatures and the local heat transfer coefficients were calculated by the method shown in Ghajar and Kim (2006). In these calculations, the axial conduction was assumed negligible (RePr > 2,800 in all cases), but peripheral and radial conduction of heat in the tube wall were included. In addition, the bulk fluid temperature was assumed to increase linearly from the inlet to the outlet. Also, the dimensionless numbers, such as Reynolds, Prandtl, Grashof, and Nusselt numbers were computed by the computer program developed by Ghajar and Kim (2006). The Reynolds number range for this study was around 800 to 13000. Heat balance errors were calculated for all experimental runs by taking a percent difference between two methods of calculating the heat addition. The product of the voltage drop across the test section and the current carried by the tube was the primary method, while the fluid enthalpy rise from inlet to exit was the secondary method. In all cases the heat balance error was less than 10%.

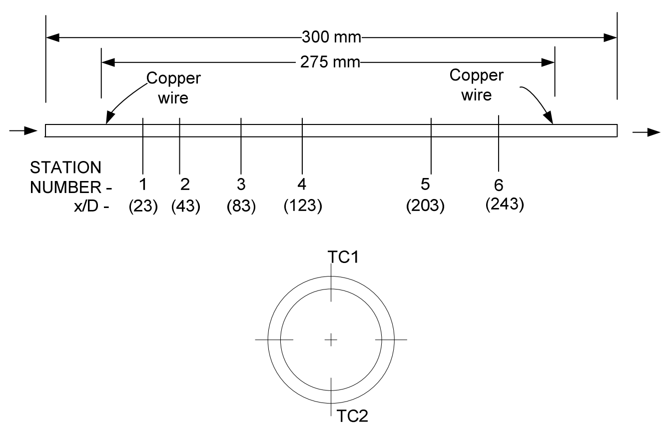

Figure 4: Arrangement of the thermocouples on the test section.

For the pressure drop measurements, based on Ghajar et al. (2010a), careful attention was paid to the sensitivity of the diaphragms of the pressure transducer. From the manufacturer, the accuracy of the Validyne pressure transducer is given as ±0.25% of the full scale reading of each diaphragm used. In this study, it was confirmed again that different ranging diaphragms would generate different results even in the same Reynolds number range. To ensure the measurement accuracy, a suitable diaphragm was selected based on the Reynolds number range. Calibrations for pressure transducer were performed before each test run. For the calibration purpose, several high accuracy WIKA gauges were used and the pressure reading uncertainty was estimated at ±1.0%.

For data acquisition, a National Instruments SCXI-1000 data collecting system was used. All digital signals from the flow meters, thermocouples, and pressure transducer were acquired and recorded by the Windows-based PC with a self-developed LabView program.

The uncertainty analyses of the overall experimental procedures using the method of Kline and McClintock (1953) showed that there is a 16% uncertainty for the heat transfer coefficient calculations and a 5% uncertainty for the friction factor calculations.

RESULTS AND DISCUSSION

To verify the new experimental setup, experiments for 2000μm stainless steel tube were conducted first. Figure 5 shows the comparison of 2000μm tube heat transfer data with the data of Ghajar and Tam (1994) for a 15800μm stainless steel tube with a square-edged inlet. The square-edged inlet data was used because the inlet of this study was also similar to the square-edged inlet type. Since the deviations between the two data sets were below 10%, the experimental setup and the heat transfer data were confirmed to be reliable. It should be noted that the parallel shift from the classical fully developed value of Nu = 4.364 for the uniform wall heat flux boundary condition in the laminar region is due to the buoyancy effect.

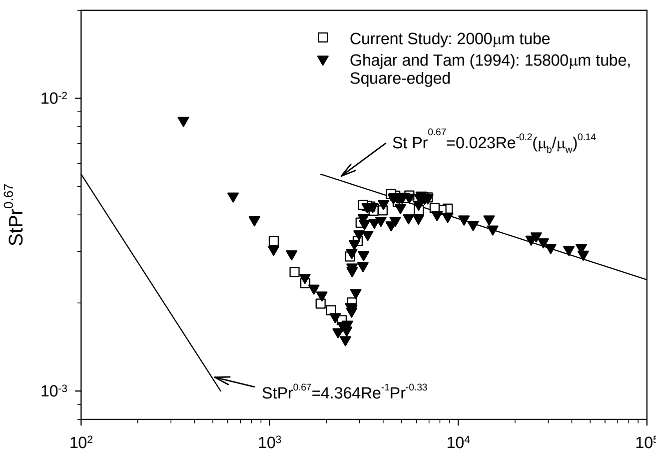

Figure 5: Comparison of present heat transfer data for the 2000μm diameter stainless steel tube with experimental data of Ghajar and Tam (1994) at x/D of 200.

Base on the careful consideration of the sensitivity of pressure transducer, the measurements of friction factor were also verified by comparing the 2000μm tube friction factor data with the classical friction factor equations for laminar and turbulent flows. As it can be seen from Figure 6, the 2000μm tube friction factor data compared very well with the classical fully-developed friction factor equations in the laminar ($f = 64/Re$) and turbulent (Blasius equation, $f = 0.316/Re^{0.25}$) regions. Figure 6 also shows that the start and end of transition were at Reynolds numbers of around 1400 and 3900, respectively. The start of transition Reynolds number of 1400 was based on the data point just leaving the laminar line, $f=64/Re$. The end of transition Reynolds number of 3600, was based on the first data point from the transition region to reach the turbulent line, $f = 0.316/Re^{0.25}$. Owing to the sharp inlet effect, the start of transition is much earlier than the typical transition Reynolds number of 2300. In Figure 6, the overall friction factor trend over the entire flow regime, especially the transition region, compared well with the experimental data of Ghajar et al. (2010a) for a stainless steel tube with a comparable diameter of 2083μm. Hence, the entire experimental setup for the pressure drop measurements was verified to be reliable.

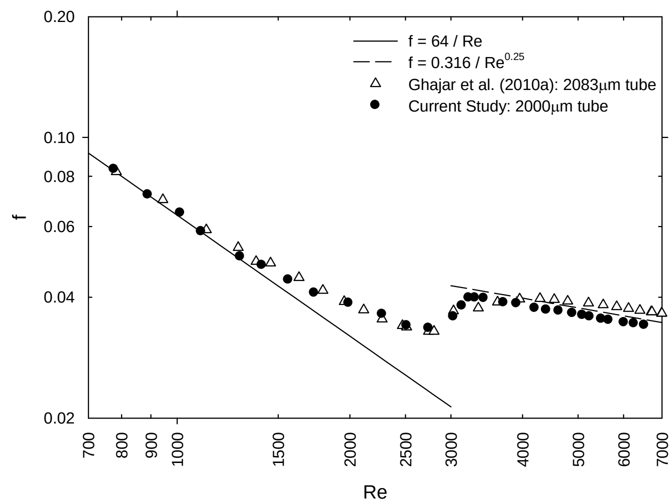

Figure 6: Comparison of present friction factor data for the 2000μm diameter stainless steel tube with classical equations and experimental data of Ghajar et al. (2010a).

After the verifications of the experimental setup, simultaneous heat transfer and pressure drop measurements and isothermal pressure drop measurements for the 1000μm micro-tube and 2000μm macro-tube were conducted. The results are shown in Figure 7 for heat transfer and Figure 8 for friction factor. As seen from these figures, the start and end of transition for heat transfer (with uniform wall heat flux boundary condition) and friction factor (with isothermal and uniform wall heat flux boundary conditions) in the 1000μm micro-tube and the 2000μm macro-tube were established.

The transition Reynolds numbers for the heat transfer and friction factor are summarized in Tables 1 and 2, respectively. From Figure 7, the start of the transition region for heat transfer was determined to be the first point from the laminar line which is parallel to the classical laminar flow line of Nu=4.364 that followed the "S" shaped curve. The end of transition region was defined as the first point that landed on the turbulent line that was parallel to the line expressed by $StPr^{0.67}=0.023Re^{-0.2}(\mu_b/\mu_w)^{0.14}$, the Sieder and Tate correlation (1936). Regarding to the start and end of the transition region for friction factor, from Figure 8, the start of transition region was defined as the first point that left the laminar line ($f = 64/Re$), and the end of the transition region was defined as the first point that landed on the turbulent line (Blasius equation, $f = 0.316/Re^{0.25}$).

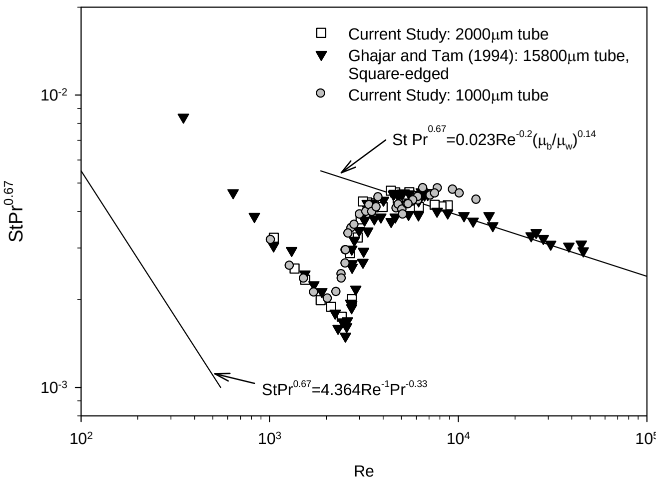

Figure 7: Heat transfer characteristics for the macro- and micro-tubes at x/D of 200.

For heat transfer, as shown in Figure 7 and Table 1, in the laminar region, the heat transfer characteristics for the 15800 μm, 2000μm and 1000μm tubes were identical. From the figure, it was observed that the transition Reynolds number range of the 2000μm tube was nearly the same as that of the 15800μm tube. However, as shown in Table 1, the lower and upper transition Reynolds numbers of the micro-tube were 2042 and 7809 which were different from the 2000μm macro-tube values (Re=2411 and 8140). From these results it appears that the start and end of the transition region for the 1000μm micro-tube is lower than that of macro-tubes and as the diameter of the tube increases, the start and end of the transition region is delayed.

Referring to Figure 7, it was observed that the heat transfer behavior from the upper transition region to the turbulent region for the macro- and micro-tubes was different. Around Reynolds number of 8,000 the macro-tube data followed the Sieder and Tate correlation (1936) for the turbulent region. However, the micro-tube data around the same Reynolds number ($Re \approx 8000$) continued to increase past the Sieder and Tate turbulent line and then followed a line parallel to the Sieder and Tate's turbulent line. This increase in the Colburn j factor ($St\,Pr^{0.67}$) and the up ward parallel shift from the Sieder and Tate correlation in the turbulent region was likely caused by the rough inner surface. According to the reviews by Krishnamoorthy et al. (2007) and Young and Kandlikar (2008), they stated that the micro-tube heat transfer data could be higher than the prediction of the classical macro-scale correlations. In turbulent region, several studies such as Celeta et al. (2002), Zhao and Liu (2006), and Liu et al. (2007) showed that the micro-tube experimental data exhibited higher Nusselt numbers than the classical correlations and therefore, the data of this study agreed with their observation. To further enrich the results, tubes with different diameters and surface roughness values should be employed in the future studies.

Table 1: Start and end of transition for heat transfer of macro- and micro- tubes at x/D of 200 (see Fig. 7).

Heat Transfer				
Tube, Condition	Re_{start}	$StPr^{0.7}$	Re_{end}	$StPr^{0.7}$
Macro-tube, Ghajar and Tam (1994): 15800μm Stainless Steel Tube (Square-edged)	2524	1.5e-3	8791	3.98e-3
Macro-tube, Current Study: 2000 μm Stainless Steel Tube	2411	1.7e-3	8140	4.16e-3
Micro-tube, Current Study: 1000 μm Stainless Steel Tube	2042	2.0e-3	7809	4.79e-3

Table 2: Start and end of transition for friction factor of macro- and micro- tubes at x/D of 200 (see Fig. 8).

Friction Factor				
Tube, Condition	Re_{start}	f	Re_{end}	f
Macro-tube, Isothermal Ghajar et al. (2010a): 2083μm Stainless Steel Tube	1455	4.87e-2	3954	3.96e-2
Macro-tube, Isothermal Current Study: 2000μm Stainless Steel Tube	1405	4.81e-2	3704	3.88e-2
Micro-tube, Isothermal Current Study: 1000 μm Stainless Steel Tube	1874	3.57e-2	3189	4.10e-2
Micro-tube, Heating Current Study: 1000 μm Stainless Steel Tube	1649	3.74e-2	3289	4.14e-2

For the friction factor under isothermal condition, as seen in Figure 8, the laminar and turbulent friction factors for the1000μm micro-tube exhibited the same behavior as the macro-tube data of the current study and Ghajar et al. (2010a). Referring to Table 2, the start and end of transition for the 2000μm macro-tube was nearly the same as the 2083μm macro-tube of Ghajar et al. (2010a). For the isothermal case, as shown in Table 2, the lower and upper transition Reynolds numbers of the 1000μm micro-tube were 1874 and 3189 which were different from the 2000μm macro-tube values (Re=1405 and 3704). In the study of Ghajar et al. (2010b), transition Reynolds numbers for 1000μm tubes with different inner surface roughness were measured and it was observed that the increase of roughness induced the narrower transition range. Therefore, the narrower transition range was concluded to be caused by roughness. Results in Table 1 also indicate that for the isothermal case, the decrease in the tube diameter from 2000μm to 1000μm delayed the onset of transition. This is also consistent with the results of Ghajar et al. (2010a) for tube diameters ranging from 2083 to 667μm.

For friction factor under heating condition, as seen in Figure 8, the laminar friction factor for the micro-tube was shown to be slightly less than the isothermal one. The reduction of friction factor under heating condition was caused by the decrease in the viscosity due to the temperature increase near the tube wall. Also, for the micro-tube, it was observed that heating delayed the start of transition. However, heating did not affect the end of the transition. Moreover, heating did not influence the friction factor in the transition and turbulent regions.

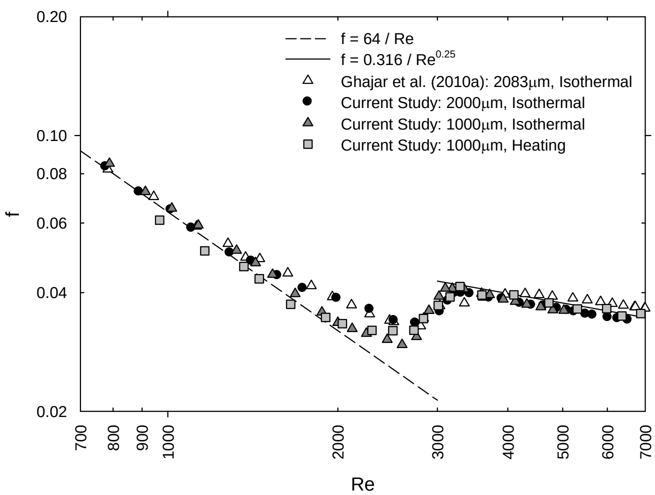

Figure 8: Friction factor characteristics for the macro- and micro-tubes at x/D of 200 under isothermal and heating boundary conditions.

CONCLUDING REMARKS

In this study, an experimental setup was designed and verified for the simultaneous measurements of heat transfer and pressure drop (friction factor) in horizontal micro- and macro-tubes under uniform wall heat flux boundary condition in all flow regimes (laminar-transition-turbulent). To verify the new experimental setup, experiments for 2000μm tube were conducted first.

For heat transfer, it was concluded that the micro-tube tested (1000μm) had an earlier start and end of the transition Reynolds numbers compared to the macro-tube (2000μm and 15800μm). It was also observed that in the turbulent region, due to the effect of roughness, the micro-tube experiences a higher rate of heat transfer.

For friction factor under isothermal condition, it was concluded that the 1000μm micro-tube had a narrower transition range due to the roughness compared to the 2000μm macro-tube. Also the decrease in the tube diameter from 2000 μm to 1000μm delayed the onset of transition.

For friction factor under heating condition, it was concluded that heating for micro-tube reduces the laminar friction factor and delays the start of transition. However, heating did not affect the end of transition.

For the micro-tube, the increase in the heat transfer in the turbulent region was likely caused by the rough inner surface. To further enrich the results, tubes with different diameters and surface roughness values should be employed in the future studies.

ACKNOWLEDGMENTS

This research is supported by the Fundo para o Desenvolvimento das Ciencias e da Tecnologia under project no. 033/2008/A2 and the Institute for the Development and Quality, Macau.

NOMENCLATURE

f fully developed friction factor coefficient (Darcy friction factor), ($=2\cdot D\cdot\Delta P / \rho\cdot L\cdot V^2$), dimensionless

c_p specific heat of the test fluid evaluated at T_b, J/(kg·K)

D inside diameter of the test section (tube), m

h fully developed peripheral heat transfer coefficient, W/(m^2·K)

k thermal conductivity, W/(m^2·K) evaluated at T_b, W/(m·K)

L length of the test section (tube), m

Nu local average or fully developed peripheral Nusselt number ($= h\cdot D / k$), dimensionless

Pr local bulk Prandtl number ($=c_p\cdot\mu_b/ k$), dimensionless

Ra surface roughness, μm

Re local bulk Reynolds number ($=\rho\cdot V\cdot D/\mu_b$), dimensionless

St local average or fully developed peripheral Staton number [$=Nu / (Pr\cdot Re)$], dimensionless

T_b local bulk temperature of the test fluid, ºC

T_w local wall temperature inside wall temperature, ºC

V average velocity in the test section, m/s

x local axial distance along the test section from the inlet, m

Greek Symbols

ΔP pressure difference, Pa

μ_b absolute viscosity of the test fluid evaluated at T_b, Pa·s

μ_w absolute viscosity of the test fluid evaluated at T_w, Pa·s

ρ density of the test fluid evaluated at T_b, kg/m^3

ε roughness height, m

REFERENCES

Choi, S. B., Barron, R. F., and Warrington, R. O., 1991, " Fluid Flow and Heat Transfer in Micro-tubes," Proceedings of Winter Annual Meeting of the ASME Dynamic Systems and Control Division, Atlanta, GA, Vol. 32, pp. 123-134.

Celeta, G. P., Gumo, M., Guglielmi, M., and Zummo, G., 2002, "Experimental Investigation of Hydraulic and Single Phase Heat Transfer in 0.130 mm Capillary Tube," Microscale Thermaophysical Engineering, Vol. 6, pp. 85-97.

Celata, G. P., 2004, “Single-Phase Heat Transfer and Fluid Flow in Micropipes,” Heat Transfer Engineering, Vol. 25, pp. 13-22.

Celeta, G.P., Cumo, M., McPhail, S., Zummo, G., 2006, “Characterization of fluid dynamic behavior and channel wall effects in micro-tube,” International Journal of Heat and Fluid Flow, Vol. 27, pp. 135-14

Ghajar, A. J. and Tam, L. M., 1994, “Heat transfer measurements and correlations in the transition region for a circular tube with three different inlet configurations”, Experimental Thermal and Fluid Science, Vol. 8, No. 1, pp. 79-90.

Ghajar, A. J. and Kim, J., 2006, “Calculation of local inside-wall convective heat transfer parameters from measurements of the local outside-wall temperatures along an electrically heated circular tube,” Heat Transfer Calculations, edited by Myer Kutz, McGraw-Hill, New York, NY, pp. 23.3-23.27.

Ghajar, A. J., Tang, C. C., Cook, W. L., 2010a, “Experimental Investigation of Friction Factor in the Transition Region for Water Flow in Mini-tubes and Micro-tubes,” Heat Transfer Engineering, vol. 31, no. 8, pp. 646-657.

Ghajar, A. J., Tam, L. M., Tam, H. K., Wen, Q., 2010b, “The Effect of Inner Surface Roughness on Friction Factor in Horizontal Micro-tubes,” Proceedings of the 2nd International Conference on Mechanical and Electronics Engineering (ICMEE 2010), , Vol. 1, pp. 59-63, Kyoto, Japan. August 1-3, 2010.

Hestroni, G., 2005, “Heat Transfer in Microchannels: Comparisons of Experiments with Theory and Numerical Results,” International Journal of Heat and Mass Transfer, Vol.48, No. 25 – 26, pp. 5580 – 5601.

Hwang, Y. W. and Kim, M. S., 2006, “The Pressure Drop in Microtubes and the Correlation Development,” International Journal of Heat and Mass Transfer, vol. 49, no. 11−12, pp. 1804−1812.

Kandlikar, S. G., Joshi, S., and Tian, S., 2003, “Effect of Surface Roughness on Heat Transfer and Fluid Flow Characteristics at Low Reynolds Numbers in Small Diameter Tubes.” Heat Transfer Engineering, vol. 24, no. 3, pp. 4-16.

Kline, S. J., and McClintock, F. A., 1953, “Describing Uncertainties in Single Sample Experiments,” Mech. Eng., vol. 75, pp. 3-8.

Krishnamoorthy, C., Rao, R. P., and Ghajar, A. J., 2007, “Single-Phase Heat Transfer in Micro-Tubes: A Critical Review,” Proceedings of the 2007 ASME-JSME Thermal Engineering Summer Heat Transfer Conference, Vancouver, British Columbia, Canada, July 8-12.

Li, Z. X., Du, D. X., and Guo, Z. Y., 2003, “Experimental Study on Flow Characteristics of Liquid in Circular Microtubes,” Nanoscale and Microscale Thermophysical Engineering, vol. 7, no. 3, pp. 253−265.

Liu, Z. G., Liang, S. Q., and Takei, M., 2007, “Experimental Study on Forced Convective Heat Transfer Characteristics in Quartz microtube,” International Journal of Thermal Sciences, Vol. 46, pp. 139-148.

Mala, G. M., Li, D. Q., 1999, “Flow characteristics of water in micro-tubes,” International Journal of Heat and Fluid Flow, Vol. 20, pp. 142-148.

Morini, G. L., 2004, “Single-Phase Convective Heat Transfer in Microchannels: A Review of Experimental Results,” International Journal of Thermal Sciences, Vol. 43, pp. 631-651.

Obot, N. T., 2000, “Towards a Better Understanding of Friction and Heat/Mass Transfer in Microchannels – A Literature Review,” Proceedings of the International Conference on Heat Transfer and Transport Phenomena in Microscale, Banff, Canada, October 15 – 20.

Palm, B., 2001, “Heat Transfer in Microchannels,” Microscale Thermophysical Engineering, Vol. 5, pp. 155-175.

Papautsky, I., Ameel, T., and Frazier, A. B., 2001, “A Review of Laminar Single Phase Flow in Microchannels,” Proceedings of ASME International Mechanical Engineering Congress and Exposition, pp. 3067-3075, Vol. 2,New York, NY, November 11 – 16, 2001.

Rands, C., Webb, B. W. and Maynes, D., 2006, “Characterization of transition to turbulence in microchannels,” International Journal of Heat and Mass Transfer, Vol. 49, pp. 2924-2930.

Rostami, A.A., Majumdar, A.S., and Saniei, N., 2002, “Flow and Heat Transfer for Gas Flowing in Microchannels: A review,” Heat and Mass Transfer, Vol. 38, pp. 359-367.

Sobhan, C. B. and Garimella, S.V., 2001, “A Comparative Analysis of Studies on Heat Transfer and Fluid Flow in Microchannels,” Microscale Thermophysical Engineering, Vol. 5, pp. 293-311.

Sieder, E. N. and Tate, G. E., 1936, “Heat Transfer and Pressure Drop in Liquids in Tubes,” Ind. Eng. Chem., Vol. 28, pp. 1429-1435.

Tam, H. K. Tam, L. M., Ghajar, A. J., and Chu W. W., 2010, “Experimental Analysis of the Single-Phase Heat Transfer and Friction Factor inside the Horizontal Internally Micro-Fin Tube,” Proceedings of the 2nd International Conference on Mechanical and Electronics Engineering (ICMEE 2010), , Vol. 1, pp.44-48, Kyoto, Japan. August 1-3, 2010.

Tang, G. H., Li, Z., He, Y. L., and Tao, W. Q., 2007, “Experimental Study of Compressibility, Roughness and Rarefaction Influences on Microchannel Flow,” International Journal of Heat and Mass Transfer, vol. 50, no. 11−12, pp. 2282−2295.

Yang, C. Y., and Lin, T. Y., 2007, “Heat transfer characteristics of water flow in micro-tubes,” Experimental Thermal and Fluid Science, Vol. 32, pp. 432-439.

Young, P. L. and Kandlikar, S. G., 2008, “Surface Roughness Effects on Heat Transfer in Microscale Single Phase Flow: A Critical Review,” Proceedings of the Sixth International ASME Conference on Nanochannels, Microchannels and Minichannels (ICNMM2008), June 23-23, 2008, Darmstadt, Germany.

Yu, D., Warrington, R., Barron, R., and Ameel, T., 1995, " Experimental and Theoretical Investigation of Fluid Flow and Heat Transfer in Microtubes," Proceedings of the 1995 ASME/JSME Thermal Engineering Joint Conference, Maui, HI, vol. 1, pp. 523−530.

Zhao, Y., and Liu, Z., 2006, "Experimental studies on Flow Visualization and Heat Transfer Characteristics in Micro-tubes," Proceeding of the 13th International Heat Transfer Conference, Sydney, Australia, MIC-12.

